molecules

MDPI

Article

A Benzil- and BODIPY-Based Turn-On Fluorescent Probe for Detection of Hydrogen Peroxide

Yunxia Wang [1,2], Ye Liu [3,4], Bo Liu [3,4], Yihua Yuan [3,4], Lixia Wei [3,4], Mingxiu Wang [5,*] and Zhe Chen [3,4,*]

1 Department of Laboratory Science, Shanxi Medical University, Taiyuan 030001, China
2 The Sixth Hospital of Shanxi Medical University (General Hospital of Tisco), Taiyuan 030001, China
3 School of Forensic Medicine, Shanxi Medical University, Jinzhong 030600, China
4 Key Laboratory of Forensic Toxicology of Ministry of Public Security, Jinzhong 030600, China
5 School of Public Health, Shanxi Medical University, Taiyuan 030001, China
* Correspondence: wangmingxiu0818@163.com (M.W.); chenzhe0322@163.com (Z.C.)

Abstract: Faced with rising threats of terrorism, environmental and health risks, achieving sensitive and selective detection of peroxide-based explosives (PEs) has become a global focus. In this study, a turn-on fluorescent probe (BOD) based on benzil (H_2O_2-recognition element) and 4,4-difluoro-4-bora-3*a*,4*a*-diaza-*s*-indacene (BODIPY) derivative (fluorophore) was developed to sensitively and specifically detect hydrogen peroxide (H_2O_2). The synthesized BOD had a very weak fluorescence due to intramolecular donor-excited photo-induced electron transfer (*d*-PET) effect; however, it could emit a strong fluorescence since H_2O_2 selectively oxidized the benzil moiety and released free BODIPY fluorophore (BOD-COOH). As a result, the proposed BOD detected H_2O_2 in linear detection ranged from 25 to 125 μM with a detection limit of 4.41 μM. Meanwhile, the proposed BOD showed good selectivity toward H_2O_2, which is not affected by other common reactive oxygen species (ROS) and ions from explosive residues. In addition, a blue shift from 508 to 498 nm was observed in the absorption spectra upon addition of H_2O_2. More importantly, the BOD was successfully applied for rapid detection of H_2O_2 vapor with good sensitivity (down to 7 ppb), which holds great potential for practical use in public safety, forensic analysis and environmental monitoring.

Keywords: turn-on fluorescence; benzil; BODIPY; hydrogen peroxide (H_2O_2); vapor detection

check for updates

Citation: Wang, Y.; Liu, Y.; Liu, B.; Yuan, Y.; Wei, L.; Wang, M.; Chen, Z. A Benzil- and BODIPY-Based Turn-On Fluorescent Probe for Detection of Hydrogen Peroxide. *Molecules* **2024**, *29*, 229. https://doi.org/10.3390/molecules29010229

Academic Editors: Barbara Panunzi and Haidong Li

Received: 22 November 2023
Revised: 15 December 2023
Accepted: 29 December 2023
Published: 31 December 2023

Copyright: © 2023 by the authors. Licensee MDPI, Basel, Switzerland. This article is an open access article distributed under the terms and conditions of the Creative Commons Attribution (CC BY) license (https://creativecommons.org/licenses/by/4.0/).

1. Introduction

In recent years, development of simple, sensitive and selective methods for the detection of explosives has become an increasingly critical public concern with rising threats in terrorism, homeland security and environmental pollution. In particular, among the conventional explosives, PEs have attracted widespread attention due to their easy synthesis and high explosive power [1]. However, compared to nitroaromatic explosives, it is difficult to detect PEs because of their own characteristics of lack of nitro groups as well as minimal UV-vis absorption and non-fluorescence [2]. It is well known that H_2O_2 has a dual role as a starting synthetic material and a decomposition product of PEs, making it a signature compound for detecting PEs [3]. Thus, achieving highly selective and sensitive detection of H_2O_2 is of great significance in effective monitoring and early warning of PEs.

Currently, a variety of analytical methods have been developed for the sensitive detection of H_2O_2, including mass spectrometry [4], electrochemical detection [5], colorimetric and fluorimetric assay [6–8]. Among them, fluorescence-based probes are the most preferred methods due to their low cost, rapid response, high sensitivity and selectivity [9,10]. Usually, boronate ester chromophore-based fluorescent probes are used based on the cleavage of the boronate group by H_2O_2, leading to an increase in fluorescence intensity [11–13]. However, these probes were reported to be susceptible to nitric oxide (NO), meaning the detection result can be disturbed by NO that decomposed by the nitro-aliphatic explosives [14]. Therefore, in order to improve the selectivity for PE detection, it is crucial to

ensure that the designed probes should be secured from disturbances like nitro-aliphatic and nitro-aromatic explosives as well as their decomposed products. Since Nagano et al. developed a novel fluorescence probe based on benzil chemistry and PET strategy to detect H_2O_2 in 2011 [15], many benzil chemistry-based probes have been designed for detection of H_2O_2 with a good reaction rate and high specificity [16,17].

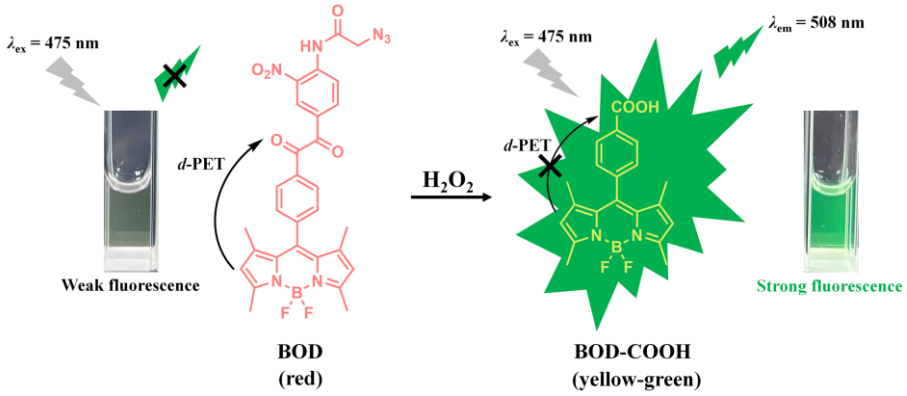
As of recently, fluorescent probes based on BODIPY fluorophores hold great promise in explosive detection due to BODIPY's outstanding photophysical properties, such as high quantum yield and good photo stability [18]. By conjugating the electron-donating group (EDG) or the electron-withdrawing group (EWG) to BODIPY, its photophysical properties can be fine-tuned through PET effect and charge-transfer intersystem crossing (ISC) process, resulting in an increase or suppression of fluorescence emission, which can be used for the construction of turn-on or turn-off fluorescent probes [15–20]. Consequently, the combination of benzil chemistry and BODIPY fluorophores can be an appropriate candidate strategy for development of fluorescent probes to detect H_2O_2. For example, Li et al. developed a turn-on fluorescent probe (*m*-NBBD) for the visual detection of H_2O_2 vapor with high sensitivity and specificity based on BODIPY combined with benzil moiety [21]. Recently, in our previous study, a cancer cell-targeting fluorescence turn-on probe based on a benzil group and a BODIPY derivative was designed for detecting H_2O_2 in biological systems, showing a high selectivity that can distinguish H_2O_2 from common ROS [22]. As a consequence, and inspired by the excellent selective response of benzil toward H_2O_2 and great fluorescence features of BODIPY, in this study, we designed a turn-on fluorescent probe (BOD) for the detection of H_2O_2 and H_2O_2 vapor by combining the merits of benzil and BODIPY.

It was hypothesized that the proposed BOD could show almost no fluorescence owing to fluorescence quenching via the *d*-PeT process. Upon H_2O_2 recognition, benzil could transform to benzoic acid, followed by the release of BODIPY dye, resulting in a fluorescence increment. Consequently, H_2O_2 could be evaluated by measuring the BODIPY fluorescence, where benzil acted as the recognition group and BODIPY acted as the fluorophore. Meanwhile, the detection solution color changed from red to yellow-green, displaying potential for colorimetric assay. More importantly, BOD was further applied for the detection of H_2O_2 vapor, which brought significant implications for the practice of PE detection.

2. Results and Discussion

2.1. Principle of the Benzil- and BODIPY-Based H_2O_2 Assay

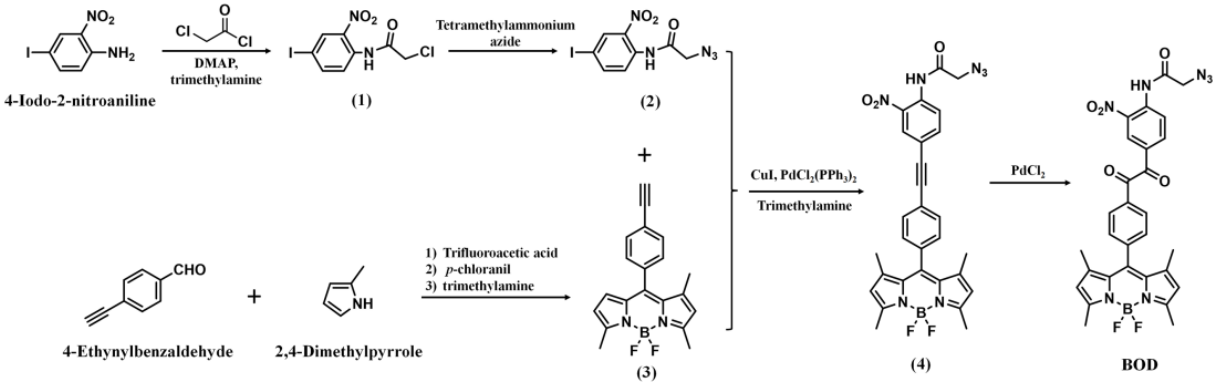
In this work, a benzil- and BODIPY-based turn-on fluorescent probe that employed benzil as H_2O_2-recognition group and BODIPY as fluorophore for the detection of H_2O_2 as well as the recognition mechanism of the proposed fluorescent assays is developed and depicted in Scheme 1. Initially, the designed BOD was almost non-emissive, which was attributed to the occurrence of the d-PET effect from BODIPY fluorophore to nitrobenzene [15,22]. In contrast, in the presence of H_2O_2, the benzil moiety could be specifically recognized and oxidized by H_2O_2, and a BODIPY derivative (BOD-COOH) could be formed and subsequently released, resulting in a turn-on fluorescence signal. Similar working principle had also been reported previously by many researchers [17,23]. Additionally, the detection solution underwent a visual color change from red (BOD) to yellow-green (BOD-COOH), which had the potential for colorimetric analysis of H_2O_2. Therefore, highly sensitive and specific detection of H_2O_2 can be successfully achieved based on the proposed benzil- and BODIPY-based probe through the fluorescence and colorimetric signal change.



Scheme 1. Schematic representation of the benzil- and BODIPY-based turn-on fluorescent probe for the detection of H_2O_2 (the X cross indicated that the process did not occur in the corresponding condition).

2.2. Synthesis and Characterizations of the BOD

As shown in Scheme 2, BOD was synthesized according to our previous study [22]. First, Compound (**1**) was synthesized through the reaction of 4-iodo-2-nitroaniline and chloroacetyl chloride in the presence of 4-dimethylaminopyridine (DMAP) and trimethylamine. Then, Compound (**1**) was reacted with tetramethylammonium azide to produce azide-modified Compound (**2**). Ethynyl-modified BODIPY of Compound (**3**) was synthesized based on the reported procedures by using 4-ethynylbenzaldehyde and 2,4-dimethylpyrrole, where the reaction was conducted with stirring under nitrogen protection [24]. Subsequently, Compound (**4**) was synthesized via Sonogashira coupling reaction of (**2**) and (**3**) by utilizing $PdCl_2(PPh_3)_2$, CuI as catalysts and trimethylamine as a base. Finally, the BOD was obtained through the oxidation of (**4**) in the presence of $PdCl_2$, and was characterized by ^{1}H NMR, ^{13}C NMR spectroscopies and high-resolution mass spectrometry (HR-MS) (Figures S1–S3).



Scheme 2. Chemical structure and synthetic route of BOD.

2.3. Feasibility of the Benzil- and BODIPY-Based H_2O_2 Assay

The feasibility of the proposed strategy was demonstrated by detecting the absorption spectra and the fluorescence response signals of BOD before and after the addition of H_2O_2. As shown in Figure 1a, the BOD probe showed its characteristic absorption profile with an absorption maximum at about 508 nm; however, the addition of H_2O_2 to BOD induced a blue shift from 508 nm to 498 nm. More importantly, the absorption spectra of the product of reaction of BOD and H_2O_2 was similar to that of the BODIPY derivative (BOD-COOH), confirming that BOD indeed reacted with H_2O_2 and generated the product BOD-COOH. Likewise, from Figure 1b, the fluorescence intensity of BOD showed an about seven-fold increment after the reaction of BOD and H_2O_2, demonstrating the formation of the BODIPY dye BOD-COOH. In addition, the HR-MS analysis of the probe BOD was

conducted before and after reacting with H_2O_2. As described in Figure 2, after incubation of the BOD and H_2O_2 for 2 h at 37 °C, the HR-MS analysis showed peaks at m/z = 367.1443 and 598.1849, which can be assigned to BOD-COOH ($[M - H]^-$) and BOD ($[M - H]^-$), respectively, further confirming the reaction of the BOD and H_2O_2, and subsequently the generation and release of the BOD-COOH product. Therefore, these results suggested that the proposed BOD probe for the detection of H_2O_2 is feasible as it can simultaneously generate fluorescence and colorimetric signal change.

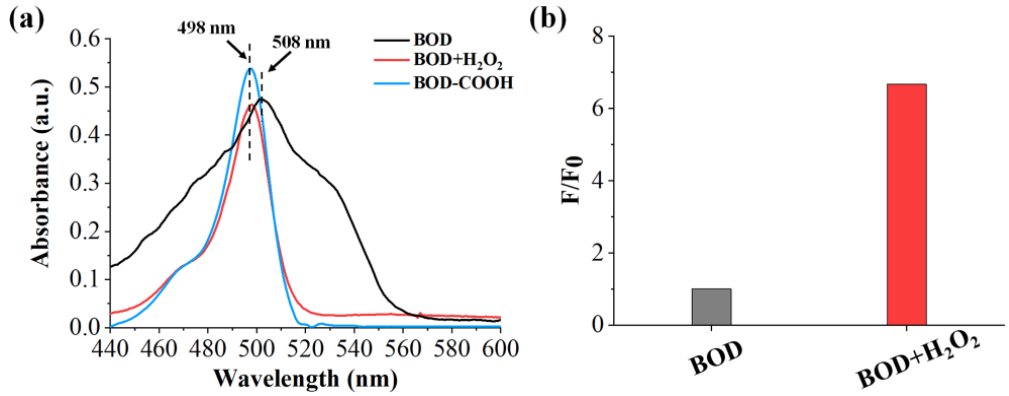


Figure 1. (**a**) UV-Vis absorption spectra of BOD before and after the addition of H_2O_2, and the BODIPY derivative (BOD-COOH) in PBS (0.1 M, pH = 7.4, 5% DMSO) buffer ([BOD] = [BOD-COOH] =10 μM, $[H_2O_2]$ = 1 mM); (**b**) Fluorescence intensity ratio of the BOD at 508 nm before (F_0) and after (F) the addition of H_2O_2 in PBS (0.1 M, pH = 7.4, 5% DMSO) buffer ([BOD] = 5 μM, $[H_2O_2]$ = 300 μM, λ_{ex} = 475 nm, λ_{em} = 508 nm).

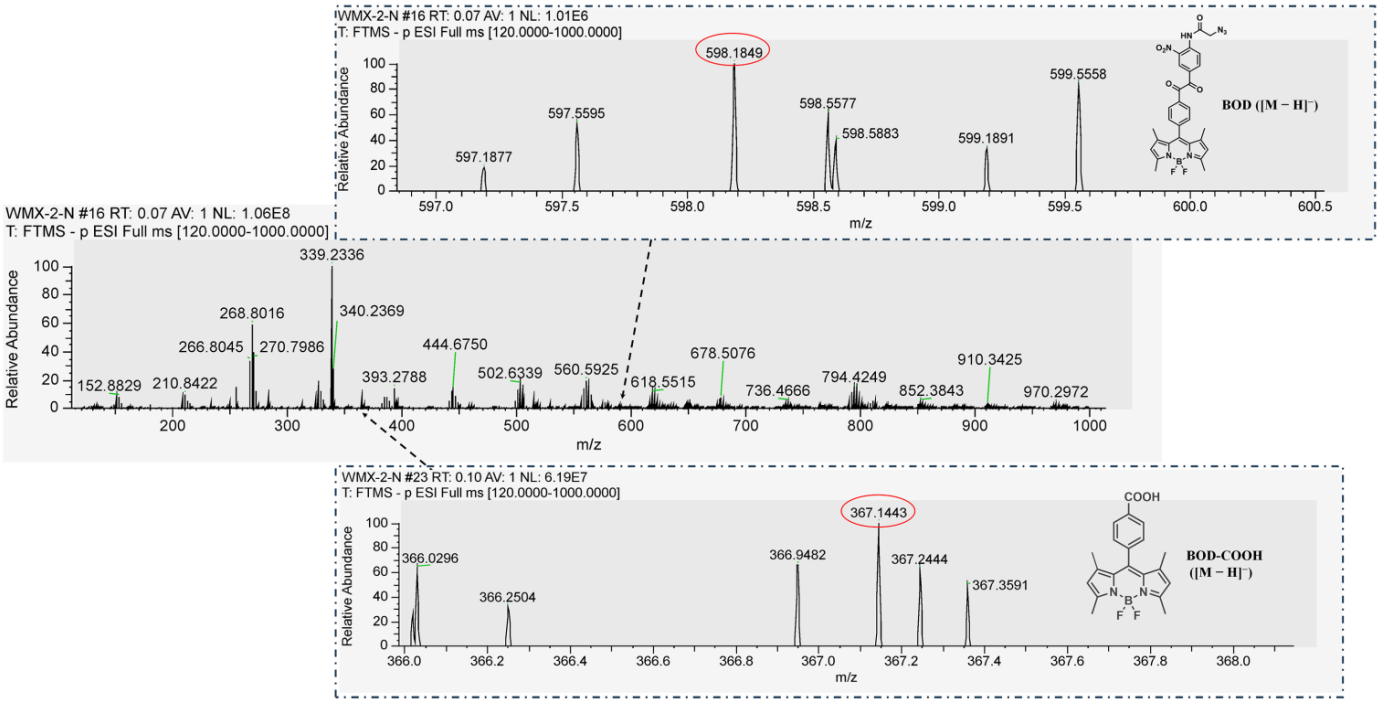


Figure 2. HR-MS analysis showing peaks of the BOD and BOD-COOH after the addition of H_2O_2 in a negative ion mode.

2.4. Optimization of the Benzil- and BODIPY-Based H_2O_2 Assay Conditions

In order to achieve good performance of the proposed probe BOD for H_2O_2 detection, detection solution, incubation time and pH of solution were optimized. It is well known that BODIPYs are sensitive to the solvent [25]; therefore, absorption and fluorescence

spectra of BOD were detected in various solvents to study if BOD could form aggregation that could subsequently affect detection efficiency. As shown in Figure S4, the absorption and fluorescence spectra measurements of BOD were determined in DMSO, PBS (0.1 M, pH = 7.4, 5% DMSO) and PBS (0.1 M, pH = 7.4, 1% DMSO) buffer, respectively. The absorption spectrum of BOD in DMSO exhibited characteristic absorption maxima at about 498 nm, while the maximum absorption peaks of BOD in PBS (0.1 M, pH = 7.4, 5% DMSO) and (0.1 M, pH = 7.4, 1% DMSO) buffer were, respectively, at about 508 and 520 nm (Figure S4a). Moskalensky et al. found that BODIPY-based dyes aggregate in water (1% DMSO), which simultaneously showed a wide absorption peak (at about 500 nm) and two fluorescence peaks [26]. As for the two fluorescence peaks, one at about 500 nm corresponded to the emission band of BODIPY in organic solvents, and one at about 650 nm corresponded to the formation of aggregation. However, the BOD only had one fluorescence peak at about 508 nm in both PBS (5% DMSO) and PBS (1% DMSO) buffer solutions (Figure S4b), indicating that the BOD was completely dissolved and no obvious aggregation phenomenon was observed in both PBS buffer solutions. In Figure S4a, the BOD shows wide absorption in the PBS buffer solution, which can be attributed to the influence of the contained benzil and azido group, and similar results have also been observed in the study of benzi by Mittal [27]. In addition, Nagano et al. designed and synthesized a library of BODIPY-based environmental polarity sensors by utilizing photoinduced electron-transfer-controlled fluorescence on/off switching. They demonstrated that the fluorescence property can be well controlled by the PET mechanism, which depends on solvent polarity [28]. Thus, as shown in Figure S4b, the fluorescence intensity of BOD in DMSO was stronger than that in the PBS (5% DMSO and 1% DMSO) buffer, which can be explained by the change in solvent polarity, resulting in a different PET process and fluorescence intensity. Consequently, the fluorescence emission of BOD was quenched mainly by the PET pathway in PBS (5% DMSO and 1% DMSO) buffer, which was not due to aggregation.

As for the optimization of incubation time, in Figure 3a, the BOD fluorescence increased on increasing the incubation time for the reaction of BOD and H_2O_2, with the fluorescence reaching a maximum at 60 min, and remained stable. Thus, 60 min was selected as the optimal incubation time.

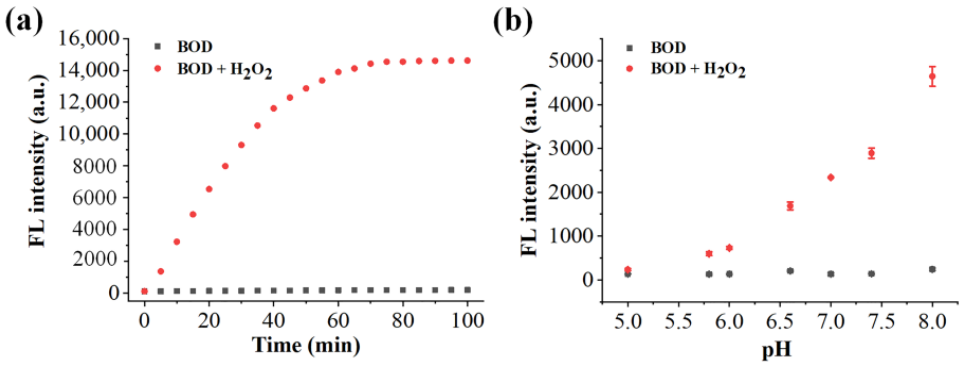


Figure 3. (**a**) Fluorescence intensity change in BOD at 508 nm after reaction with H_2O_2 for different incubation times ([BOD] = 5 μM, [H_2O_2] = 2 mM); (**b**) Fluorescence intensity change in BOD at 508 nm after reaction with H_2O_2 at different pH (error bars indicate the standard deviation of measurements (n = 3), [BOD] = 5 μM, [H_2O_2] = 1 mM).

In addition, the effect of pH was also investigated by detecting the BOD fluorescence in the presence of H_2O_2 in PBS buffer from pH 5.0 to 8.0. After reaction with H_2O_2, the BOD fluorescence was pH-dependent and rose with increasing pH value as shown in Figure 3b, which can be attributed to the deprotonation of carboxylic acid (product BOD-COOH) to form carboxylate ($-COO^-$) in alkaline solution [21]. In contrast, the fluorescence of free BOD remained stable between pH values of 5.0 and 8.0. Considering the generality of the

proposed approach, therefore, physiological pH (pH = 7.4) in PBS buffer was chosen for the following experiments.

2.5. Photostability Study of the BOD Probe

Further, the photostability of the proposed BOD probe was studied since it is vital for optical-based sensing probes. In particular, PEs were usually detected by H_2O_2 that generated by their photolysis. As a result, photostability is a critical requirement for the design of probes to detect H_2O_2. It was found that the fluorescence response of BOD remained stable in the presence of H_2O_2 upon continuous UV irradiation at 365 nm for 180 min (Figure 4), indicating great photostability of the proposed BOD.

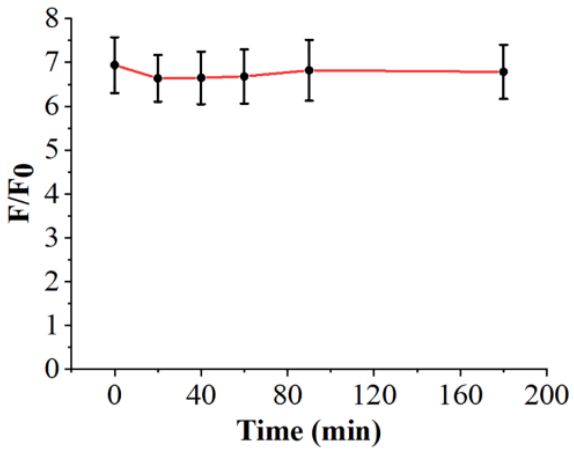


Figure 4. Photostability was evaluated by detecting the fluorescence intensity ratio of BOD at 508 nm before (F_0) and after (F) the addition of H_2O_2 upon continuous UV irradiation (2 × 8 W, emission at 365 nm) for 180 min ([BOD] = 5 μM, [H_2O_2] = 300 μM).

2.6. Sensitivity of the Benzil- and BODIPY-Based H_2O_2 Assay

In order to evaluate the H_2O_2 detection capability of the proposed BOD probe, the fluorescence spectra of the BOD were measured in the presence of H_2O_2 at different concentrations (0, 0.1, 0.2, 0.3, 0.4, 0.5, 0.7, 1, 2 mM). As the concentration of H_2O_2 increased from 0 to 2 mM, the fluorescence emission peak of BOD was gradually enhanced (Figure 5a), which was consistent with the fact that H_2O_2 could selectively oxidize the benzil moiety of BOD and generate the BODIPY fluorophore BOD-COOH, subsequently resulting in a turn-on fluorescence signal with a bright green fluorescence under UV radiation (Figure 5d, upper panel). Furthermore, it was observed that the BOD fluorescence intensity at 508 nm had a good linear correlation to the concentration of H_2O_2 in the range of 0 to 125 μM with a correlation coefficient of 0.9941 (Figure 5b), and a limit of detection (LOD) of 4.41 μM was determined according to 3σ/K (σ is the standard deviation and K is the slope of the curve of linear regression).

In addition, the colorimetric sensing ability of the proposed probe BOD was evaluated by measuring UV-vis absorption spectra of the BOD with different concentrations of H_2O_2. The results showed that the characteristic absorption peak of BOD at 508 nm disappeared upon the addition of H_2O_2, while two new peaks appeared at ~540 nm and ~498 nm (Figure 5c). And the peak at ~540 nm disappeared gradually with the increase in H_2O_2 concentration, but at the same time, the peak of BOD at ~498 nm displayed an enhancement. The generation of the new peak at ~540 nm might derive from the intermediate product of reaction between BOD and H_2O_2 [15,21]. Meanwhile, the color of the above BOD solution was clearly changed from red to yellow-green after H_2O_2 treatment with a certain concentration (Figure 5d, bottom panel). As a result, H_2O_2 can be visually detected by the naked eye when its concentration exceeds 0.5 mM.

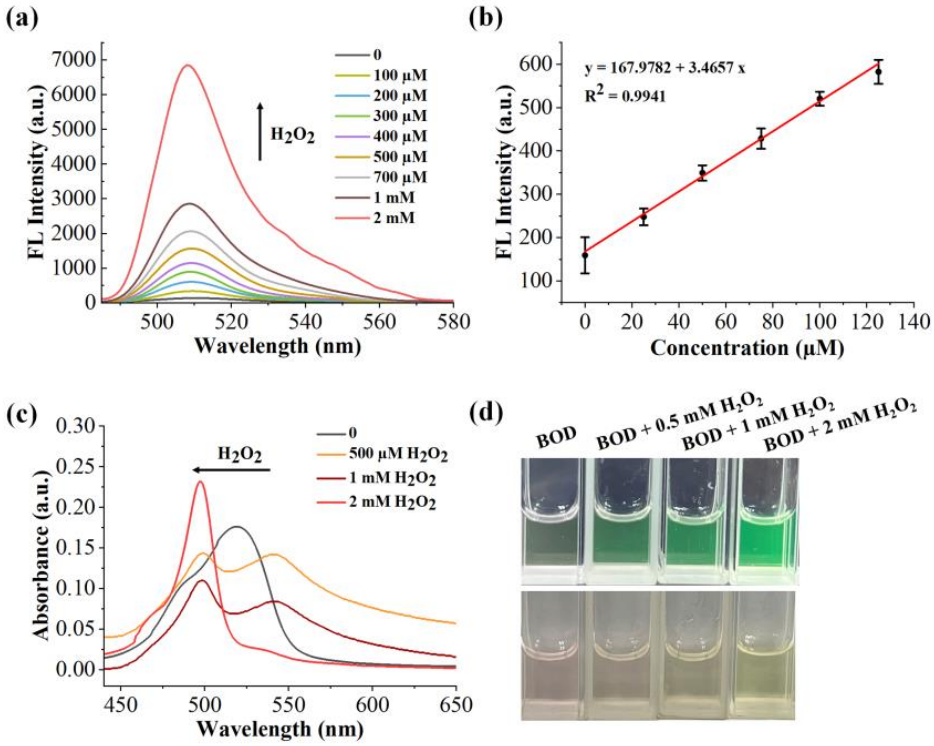


Figure 5. (**a**) Fluorescence response spectra of the proposed BOD probe with different concentrations of H_2O_2 in the range of 0–2 mM; (**b**) The relationship between the BOD fluorescence intensity at 508 nm and different concentrations of H_2O_2 in the range of 0 to 125 μM (0, 25, 50, 75, 100, 125 μM); (**c**) UV−vis absorption spectra of the BOD with different concentrations of H_2O_2; (**d**) Upper panel: the photographs of the BOD before and after addition of H_2O_2 under a UV lamp; Bottom panel: the photographs of the BOD before and after addition of H_2O_2 under visible-light irradiation. [BOD] = 5 μM.

2.7. Selectivity of the Benzil- and BODIPY-Based H_2O_2 Assay

Selectivity is another important factor for fluorescent probes with reliable and high detection efficiency; therefore, the specificity of the BOD was then investigated by comparing H_2O_2 with other common ROS (superoxide radical ($O_2^{\bullet-}$), $^1O_2$, •OH, •NO, $ONOO^-$, tert-butoxy radical (•O^{t}Bu) and tert-butyl hydroperoxide (TBHP)) and common ions from explosive residues (NO_2^-, NO_3^- and ClO^-). As displayed in Figure 6, only H_2O_2 was able to induce the highest fluorescence response when compared with other ROS and interferences from the explosive residues. The results indicated that the proposed BOD is capable of detecting H_2O_2 with high specificity.

Additionally, reduction in azide-functionalized fluorophores to amines can be utilized for the detection of hydrogen sulfide (H_2S) [29–32]; therefore, the BOD was treated with H_2S to further study whether there is any possible interference of H_2S with the detection performance of the proposed strategy. As shown in Figure S5a, the BOD showed a relatively weak fluorescence emission in the presence of H_2S (Figure S5a), while the introduction of H_2O_2 induced a large fluorescent enhancement (about 12-fold) (Figure S5b). The reason for this result may be that the PET effect from BODIPY to benzil moiety still remains after the reduction in the azide group as the BOD in the study was constructed by modifying BODIPY with an azide-substituted benzil group, which cannot recover the BODIPY fluorescence, further confirming the selectivity of the proposed BOD for H_2O_2 detection.

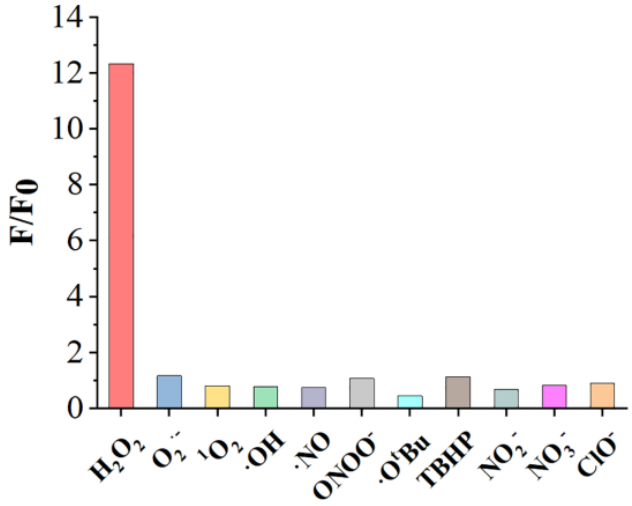


Figure 6. Selectivity assay of fluorescence responses of the BOD to H_2O_2 and other ROS ($O_2^{\bullet-}$, $^1O_2$, •OH, •NO, $ONOO^-$, •O^{t}Bu, and TBHP) and common ions from explosive residues (NO_2^-, NO_3^- and ClO^-). F was the fluorescence intensity of the BOD at 508 nm with the addition of different testing species, F_0 was the fluorescence intensity of the BOD at 508 nm without the addition of the testing species; [BOD] = 5 μM.

2.8. Detection of H_2O_2 Vapor Based on the Proposed BOD Probe

It is well known that trace detection of vapor emanated from explosives is a significant practical application for explosive monitoring. Therefore, the practical applicability of the proposed BOD probe was examined by detecting H_2O_2 vapor. We found that the BOD-coated thin-layer chromatography (TLC) plate with the image of SMU (an abbreviation of Shanxi Medical University) emitted an obvious green fluorescence under H_2O_2 vapor (Figure 7a), suggesting the success of detection of H_2O_2 vapor based on the BOD. Then, the response time of BOD toward H_2O_2 vapor was tested, as shown in Figure 7b; a bright green emission could be observed 20 min after exposure to H_2O_2 vapor and the green fluorescence increased gradually with exposure time, which can be clearly distinguished from background emission (without H_2O_2 treatment), indicating a great potential in H_2O_2 vapor rapid detection.

What is more, we studied the sensitivity of the BOD probe for the detection of H_2O_2 vapor by being exposed to different concentrations of H_2O_2 vapor from 0.8 to 31 ppb (Figure 7c). It was observed that the fluorescence emission of BOD became stronger progressively with increasing the concentration of H_2O_2, and the fluorometric change can be easily observed by the naked eye when H_2O_2 vapor concentration was above 7 ppb, suggesting the detection range of 0.8 to 31 ppb with the limit of detection of 7 ppb. All these results demonstrated the high sensitivity of the proposed probe for the detection of H_2O_2 vapor, implying the proposed assay has great potential for practical applications, especially in rapid on-site detection of PEs.

Although the proposed method showed enough sensitivity, there is still great potential to improve detection time. Nagano et al. developed a series of fluorescence probes based on benzil chemistry and photo-induced electron transfer (PET) strategy to detect H_2O_2. They found that the reactivity between benzil and H_2O_2 could be adjusted by modification of the benzene ring of benzil [15]. They synthesized five derivatives with various electron-donating or -withdrawing substituents on the benzil moiety, and the results showed that compounds with strongly electron-withdrawing groups of the cyano group and the nitro group exhibited a rapid fluorescence increase even at low concentrations of H_2O_2. In addition, they designed the probe by using the water-soluble fluorophore carboxyfluorescein. Thus, the cyano group, fluorescein and rhodamines can be utilized to construct benzil-based fluorescent probes to further optimize the measurement time for the detection of H_2O_2.

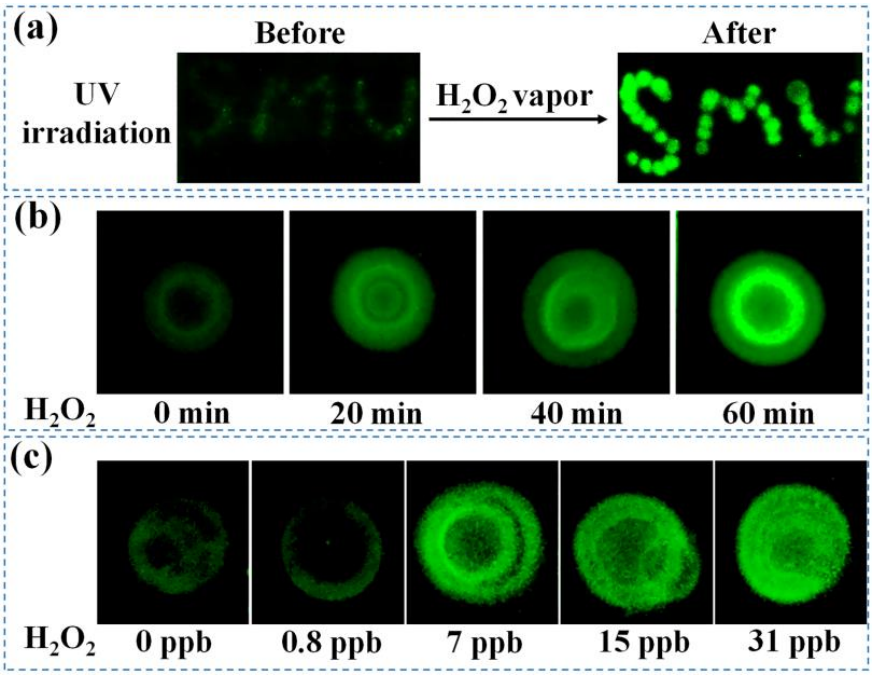


Figure 7. (**a**) The emissive response of the BOD-coated TLC plate with the image of SMU (an abbreviation of Shanxi Medical University) before and after being exposed to H_2O_2 vapor under UV irradiation (365 nm); (**b**) The emissive response of the BOD-coated TLC plate toward H_2O_2 vapor with different exposure time under UV irradiation (365 nm); (**c**) The emissive response of the BOD-coated TLC plate toward H_2O_2 with different concentrations of H_2O_2 vapor under UV irradiation (365 nm).

3. Materials and Methods

3.1. Materials

All chemicals and solvents were used as received without further purification unless specified otherwise. Chloroacetyl chloride, 4-iodo-2-nitroaniline, trifluoroacetic acid and dimethyl sulfoxide (DMSO) were purchased from Aladdin Chemical Reagent Co., Ltd. (Shanghai, China). Trimethylamine, DMAP, $PdCl_2(PPh_3)_2$, CuI and $PdCl_2$ were purchased from Sigma-Aldrich (St. Louis, MO, USA). 4-ethynylbenzaldehyde and 2,4-dimethylpyrrole were obtained from TCI (Shanghai) Development Co., Ltd. (Shanghai, China). Tetramethylammonium azide, Compounds (**1**), (**2**), (**3**) and (**4**) were synthesized according to previous procedures [20,22]. Standard solutions of NO_2^-, NO_3^- and ClO^- were purchased from Beijing Mreda Technology Co., Ltd. (Beijing, China). Silica gel TLC plates were purchased from Qingdao Ocean Chemicals (Qingdao, China). All the solvents of analytical grade were employed without further purification.

3.2. Apparatus

^1H and ^{13}C NMR spectra were recorded on a JEOL JNM-LA400. High-resolution mass spectra (HR-MS) were conducted on Q Exactive Focus MS (ThermoFisher, Waltham, MA, USA) and MALDI-TOF-MS (Bruker Autoflex III, Billerica, MA, USA).

3.3. Synthesis of BOD

$PdCl_2$ (0.023 g, 0.132 mmol) and Compound (**4**) (0.05g, 0.088 mmol) were added to 5 mL anhydrous DMSO solution, then the mixture was stirred at 65 °C for 3.5 h under a N_2 atmosphere. After cooling to room temperature, CH_2Cl_2 was added to the mixture. The mixture was subsequently washed with water and dried over $MgSO_4$. After the evaporation of solvent, the crude product was purified by a silica gel column using petroleum ether/ethyl acetate (v/v 4:1) as eluent to produce BOD as a reddish brown solid (0.027 g, 52.1% yield). ^1H NMR (400 MHz, $CDCl_3$): δ (ppm) 11.46 (s, 1H), 9.03 (d, J = 9.0 Hz, 1H),

8.93 (d, J = 1.9 Hz, 1H), 8.33 (dd, J = 8.9, 2.0 Hz, 1H), 8.15 (d, J = 8.2 Hz, 2H), 7.52 (d, J = 8.2 Hz, 2H), 6.00 (s, 2H), 4.28 (s, 2H), 2.56 (s, 6H), 1.38 (s, 6H). ^{13}C NMR (101 MHz, $CDCl_3$): δ (ppm) 191.34, 189.50, 166.29, 156.36, 142.68, 142.36, 139.12, 138.51, 136.53, 136.09, 132.68, 130.79, 130.60, 129.24, 128.31, 128.00, 122.16, 121.67, 53.36, 14.72. HR-MS (ESI): m/z, 598.1849 $[M - H]^-$, calcd for $C_{29}H_{24}BF_2N_7O_5$, 599.19.

3.4. Feasibility of the BOD-Based H_2O_2 Assay

BOD was dissolved in DMSO to make a 5 mM stock solution, and standard solution of H_2O_2 (30 wt%) was diluted with a PBS buffer to the required concentration. The experiments were performed in 200 μL of PBS buffer containing BOD and different concentrations of H_2O_2. After incubation of 60 min, the BOD absorption and fluorescence spectra were recorded using a Tecan plate reader (Tecan, Männedorf, Switzerland) with a Costar 96 Flat Bottom White plate and a Costar black bottom 96-well plate, respectively. All absorption and fluorescence spectra measurements were performed in PBS (0.1 M, pH = 7.4, 5% DMSO) buffer at 37 °C.

3.5. Sensitivity and Selectivity of the BOD-Based H_2O_2 Assay

BOD and H_2O_2 were mixed in the PBS buffer, and the final concentration of BOD was 5 μM. After being incubated with different concentrations of H_2O_2 for 60 min, the BOD fluorescence emission spectra of the mixture were measured with a Tianmei FL970 fluorescence spectrophotometer (Tianmei, Shanghai, China) (475 nm for excitation and 485–580 nm for emission). For UV-Vis absorbance spectra, the mixture was measured using a AOEA560 UV-vis spectrometer (AO YI, Shanghai, China) with a 1 cm optical path length cell.

As for the selectivity of the fluorescence assay, $O_2^{\bullet-}$, $^1O_2$, •OH, •NO, $ONOO^-$, •O^{t}Bu, TBHP, NO_2^-, NO_3^- and ClO^- were used. Based on the published procedures for the preparation of ROS [22,33–35], the ROS stock solutions were first prepared as follows. $O_2^{\bullet-}$ was prepared from the enzymatic reaction of 23.6 mU/L xanthine oxidase and 1.0 mM hypoxanthine in the presence of catalase (25 μg/mL, which is used as a scavenger of H_2O_2). $^1O_2$ was generated through the reaction of 1.0 mM OCl^- (5-fold excess) and 200 μM H_2O_2. •OH was produced by the Fenton reaction of 1.0 mM $Fe(ClO_4)_2$ with 200 μM H_2O_2 in which $Fe(ClO_4)_2$ was in excess. •O^{t}Bu was produced by reaction of 1.0 mM $Fe(ClO_4)_2$ with 200 μM TBHP. •NO was obtained from sodium nitroferricyanide. $ONOO^-$ was synthesized by the reaction of $NaNO_2$ with H_2O_2 in an acidic solution, and its concentration was determined by the absorbance peak at 302 nm. To a solution of BOD (5 μM) in a PBS (0.1 M, pH = 7.4, 5% DMSO) buffer, 500 μM H_2O_2, 500 μM of $O_2^{\bullet-}$, $^1O_2$, •OH, •NO, $ONOO^-$, •O^{t}Bu and TBHP, 100 mM of NO_2^-, NO_3^- and ClO^- were added at 37 °C, respectively. After incubation of 60 min, fluorescence intensities of the BOD were recorded at 508 nm with excitation at 475 nm (all fluorescence spectra were recorded using the Tianmei FL970 fluorescence spectrophotometer with the same detection parameters as described above).

3.6. Detection of H_2O_2 Vapor

In order to detect the H_2O_2 vapor, the BOD solution was drop-coated onto a silica gel TLC plate (2.8 (length) × 2.3 (width) cm) with about 1.0 cm radius circle and subsequently dried for 10 min. The experiment was performed by hanging the prepared BOD-coated TLC plate in the saturated vapor of H_2O_2 generated in a 100 mL bottle, where approximately 20 mL of H_2O_2 solution (diluted down to various concentrations) was put in and sealed for 12 h to reach the equilibrium vapor pressure. The equilibrium vapor pressure corresponding to a specific diluted concentration of H_2O_2 solution was deduced from the reported literatures [21,36,37]. Thus, various diluted concentrations (3.5 wt%, 1.4 wt%, 0.7 wt%, 0.35 wt%) of H_2O_2 solution were obtained by diluting the commercial 30 wt% H_2O_2 solution with pure water, which produce saturated (equilibrium) vapor pressures of H_2O_2 of 10.5 ppm, 4.0 ppm, 1.9 ppm and 1.0 ppm, respectively. Then, the above H_2O_2 solutions were diluted with water to obtain the final test vapor with lower concentrations

(0.8 ppb, 7 ppb, 15 ppb and 31 ppb). After exposure to the vapor for different time intervals, the fluorescence images of the TLC plates were obtained on a gel imaging system under the excitation at 365 nm. The H_2O_2 vapor concentration was calibrated by using the following Equation (1) since a binary system of H_2O/H_2O_2 was employed as a solution:

$$y_{H_2O_2} = \frac{Y_{H_2O_2} \times X_{H_2O_2} \times Ps_{H_2O_2}}{P}, \quad (1)$$

where y, Y, X, Ps, and P were defined as the molar fraction in the vapor phase, the activity coefficient, the molar fraction in the liquid phase, the vapor pressure of H_2O_2 (1.801 mmHg), and atmospheric pressure (1 atm), respectively [38]. Moreover, the activity coefficient of H_2O_2 was calculated from the following Equation (2) (Margules' equation):

$$Y_{H_2O_2} = e^{X_{H_2O_2}{}^2(-1.2661 + 0.2932 \times X_{H_2O})}. \quad (2)$$

After incubation, the fluorescence images of the TLC plates were obtained on gel imaging system (Bio-Rad, Hercules, CA, USA) under the excitation at 365 nm.

4. Conclusions

In summary, we developed a turn-on fluorescent probe BOD to sensitively and specifically detect H_2O_2. The proposed BOD was designed by integrating benzil moiety with BODIPY derivative, in which benzil was employed as an H_2O_2 recognition group and BODIPY was used as fluorophore. The fluorescence and absorbance emission of the BOD could be tuned by adjusting H_2O_2 concentration, so H_2O_2 can be detected through the fluorescence and colorimetric signal change with high sensitivity and selectivity. More importantly, the probe BOD exhibited fast response (down to 20 min) and high sensitivity (down to 7 ppb) for the detection of H_2O_2 vapor, providing great potential for real-time in-field detection and monitoring of PEs.

Supplementary Materials: The following supporting information can be downloaded at: https://www.mdpi.com/article/10.3390/molecules29010229/s1, Figure S1: 1H NMR spectrum of the probe BOD; Figure S2: 13C NMR spectrum of the probe BOD; Figure S3: HR-MS of the probe BOD; Figure S4: Absorption (a) and fluorescence (b) spectra measurements of BOD were determined in DMSO, PBS (0.1 M, pH = 7.4, 5% DMSO) and PBS (0.1 M, pH = 7.4, 1% DMSO) buffer, respectively. ([BOD] = 10 μM); Figure S5: (a) Fluorescence responses of the proposed BOD to H2O2 and H2S, respectively. (b) Fluorescence intensity ratio (F/F0) changes of the BOD after the addition of H_2O_2 and H_2S, respectively. F was the fluorescence intensity of the BOD at 508 nm with the addition of different targets, F_0 was the fluorescence intensity of the BOD at 508 nm without the addition of the targets. [BOD] = 5 μM, [H_2O_2] = [H_2S] = 500 μM.

Author Contributions: Conceptualization, M.W. and Z.C.; methodology, Y.W., M.W. and Z.C.; validation, Y.W., M.W. and Z.C.; formal analysis, Y.W., Y.L., B.L., Y.Y. and L.W.; investigation, Y.W., Y.L., B.L., Y.Y. and L.W.; resources, M.W. and Z.C.; data curation, Y.W., Y.L., B.L., Y.Y. and L.W.; writing—original draft preparation, Z.C.; writing—review and editing, Z.C.; visualization, Z.C.; supervision, M.W. and Z.C.; project administration, M.W. and Z.C.; funding acquisition, Z.C. All authors have read and agreed to the published version of the manuscript.

Funding: This work was supported by grants from the National Natural Science Foundation of China (No. 82101980), the China Postdoctoral Science Foundation (2022M722963), the Fundamental Research Program of Shanxi Province (No. 20210302124181), the Fund Program for the Scientific Activities of Selected Returned Overseas Professionals in Shanxi Province (No. 20220021), the Startup Foundation for Doctors of Shanxi Medical University (No. XD2037), and the Scientific and Technological Innovation Programs of Higher Education Institutions in Shanxi (No. 2021L239).

Institutional Review Board Statement: Not applicable.

Informed Consent Statement: Not applicable.

Data Availability Statement: Data are available from the authors upon reasonable request.

Conflicts of Interest: The authors declare no conflict of interest.

References

1. Schulte-Ladbeck, R.; Vogel, M.; Karst, U. Recent methods for the determination of peroxide-based explosives. *Anal. Bioanal. Chem.* **2006**, *386*, 559–565. [CrossRef] [PubMed]
2. Xu, W.; Fu, Y.; Gao, Y.; Yao, J.; Fan, T.; Zhu, D.; He, Q.; Cao, H.; Cheng, J. A simple but highly efficient multi-formyl phenol-amine system for fluorescence detection of peroxide explosive vapour. *Chem. Commun.* **2015**, *51*, 10868–10870. [CrossRef] [PubMed]
3. Xu, M.; Han, J.M.; Wang, C.; Yang, X.; Pei, J.; Zang, L. Fluorescence ratiometric sensor for trace vapor detection of hydrogen peroxide. *ACS Appl. Mater. Interfaces* **2014**, *6*, 8708–8714. [CrossRef] [PubMed]
4. Dong, B.; Hu, Z.; Xu, Q.; Liu, B.; Zhu, Q.; Guan, J.; Liu, C.; Pan, Y.; Hu, L.; Fang, J.; et al. Improving quantification of hydrogen peroxide by synchrotron vacuum ultraviolet photoionization mass spectrometry. *Combust. Flame* **2022**, *242*, 112214. [CrossRef]
5. Xing, L.; Zhang, W.; Fu, L.; Lorenzo, J.M.; Hao, Y. Fabrication and application of electrochemical sensor for analyzing hydrogen peroxide in food system and biological samples. *Food Chem.* **2022**, *385*, 132555. [CrossRef]
6. Bai, W.; Zhang, K.; Yu, S.; Zhang, J.; Jin, L. The preparation of MnO_2/BSA/CdTe quantum dots complex for ratiometric fluorescence/ T(1)-weighted MRI detection of H_2O_2. *Talanta* **2023**, *252*, 123774. [CrossRef]
7. Wang, L.; Liu, Y.; Yang, Z.; Wang, Y.; Rao, H.; Yue, G.; Wu, C.; Lu, C.; Wang, X. A ratiometric fluorescence and colorimetric dual-mode assay for H_2O_2 and xanthine based on Fe, N co-doped carbon dots. *Dye. Pigment.* **2020**, *180*, 108486. [CrossRef]
8. Su, L.; Cai, Y.; Wang, L.; Dong, W.; Mao, G.; Li, Y.; Zhao, M.; Ma, Y.; Zhang, H. Hemin@carbon dot hybrid nanozymes with peroxidase mimicking properties for dual (colorimetric and fluorometric) sensing of hydrogen peroxide, glucose and xanthine. *Mikrochim. Acta* **2020**, *187*, 132. [CrossRef]
9. Zhang, Z.; Yang, S.; Dong, B.; Kong, X.; Tian, M. Chameleon-Like Fluorescent Probe for Monitoring Interplays between Three Organelles and Reporting Cell Damage Processes through Dramatic Color Change. *Small* **2022**, *18*, e2205026. [CrossRef]
10. Xue, H.; Ge, E.; Ge, W.; Li, J.; Tian, M. Single Fluorescent Probe for Zero-Crosstalk Discrimination of Lipid Droplets and the Endoplasmic Reticulum Based on Reversible Cyclization Reaction. *Anal. Chem.* **2022**, *94*, 9158–9165. [CrossRef]
11. Fan, S.; Lai, J.; Burn, P.L.; Shaw, P.E. Solid-State Fluorescence-based Sensing of TATP via Hydrogen Peroxide Detection. *ACS Sens.* **2019**, *4*, 134–142. [CrossRef] [PubMed]
12. Qian, Y.; Xue, L.; Hu, D.; Li, G.; Jiang, H. Quinoline-based fluorescent probe for ratiometric detection of hydrogen peroxide in aqueous solution. *Dye. Pigment.* **2012**, *95*, 373–376. [CrossRef]
13. Zhang, Y.; Jiao, Z.; Xu, W.; Fu, Y.; Zhu, D.; Xu, J.; He, Q.; Cao, H.; Cheng, J. Design, synthesis and properties of a reactive chromophoric/fluorometric probe for hydrogen peroxide detection. *New J. Chem.* **2017**, *41*, 3790–3797. [CrossRef]
14. Zielonka, J.; Kalyanaraman, B. Small-molecule luminescent probes for the detection of cellular oxidizing and nitrating species. *Free Radic. Biol. Med.* **2018**, *128*, 3–22. [CrossRef] [PubMed]
15. Abo, M.; Urano, Y.; Hanaoka, K.; Terai, T.; Komatsu, T.; Nagano, T. Development of a highly sensitive fluorescence probe for hydrogen peroxide. *J. Am. Chem. Soc.* **2011**, *133*, 10629–10637. [CrossRef]
16. Purdey, M.S.; McLennan, H.J.; Sutton-McDowall, M.L.; Drumm, D.W.; Zhang, X.; Capon, P.K.; Heng, S.; Thompson, J.G.; Abell, A.D. Biological hydrogen peroxide detection with aryl boronate and benzil BODIPY-based fluorescent probes. *Sens. Actuators B Chem.* **2018**, *262*, 750–757. [CrossRef]
17. Huang, X.; Li, Z.; Liu, Z.; Zeng, C.; Hu, L. A near-infrared fluorescent probe for endogenous hydrogen peroxide real-time imaging in living cells and zebrafish. *Dye. Pigment.* **2019**, *165*, 518–523. [CrossRef]
18. Nguyen, Y.T.; Shin, S.; Kwon, K.; Kim, N.; Bae, S.W. BODIPY-based fluorescent sensors for detection of explosives. *J. Chem. Res.* **2023**, *47*, 17475198231168961. [CrossRef]
19. Erande, Y.; Chemate, S.; More, A.; Sekar, N. PET governed fluorescence "Turn ON" BODIPY probe for selective detection of picric acid. *RSC Adv.* **2015**, *5*, 89482–89487. [CrossRef]
20. Gao, J.; Chen, X.; Chen, S.; Meng, H.; Wang, Y.; Li, C.; Feng, L. The BODIPY-Based Chemosensor for Fluorometric/Colorimetric Dual Channel Detection of RDX and PA. *Anal. Chem.* **2019**, *91*, 13675–13680. [CrossRef]
21. Li, B.; Chen, J.; Xiong, Y.; Yang, X.; Zhao, C.; Sun, J. Development of turn-on fluorescent probes for the detection of H_2O_2 vapor with high selectivity and sensitivity. *Sens. Actuators B Chem.* **2018**, *268*, 475–484. [CrossRef]
22. Wang, M.; Zhang, F.; Wang, C.; Yin, N.; Wang, Y.; Qin, G.; Xu, Q.; Gong, J.; Liu, H.; Duan, X. Target-Binding Accelerated Response for Sensitive Detection of Basal H_2O_2 in Tumor Cells and Tissues via a Dual-Functional Fluorescence Probe. *Anal. Chem.* **2022**, *94*, 5962–5969. [CrossRef]
23. Peng, J.; Hou, X.; Zeng, F.; Wu, S. Fluorescent nanoprobe for in-vivo ratiometric imaging of endogenous hydrogen peroxide resulted from drug-induced organ damages. *Biosens. Bioelectron.* **2017**, *94*, 278–285. [CrossRef]
24. Schulz-Fincke, A.; Blaut, M.; Braune, A.; Gütschow, M. A BODIPY-Tagged Phosphono Peptide as Activity-Based Probe for Human Leukocyte Elastase. *ACS Med. Chem. Lett.* **2018**, *9*, 345–350. [CrossRef]
25. Rurack, K.; Kollmannsberger, M.; Daub, J. Molecular Switching in the Near Infrared (NIR) with a Functionalized Boron-Dipyrromethene Dye. *Angew. Chem. Int. Ed. Engl.* **2001**, *40*, 385–387. [CrossRef]
26. Panfilov, M.A.; Karogodina, T.Y.; Songyin, Y.; Karmatskih, O.Y.; Vorob'ev, A.Y.; Tretyakova, I.S.; Glebov, E.M.; Moskalensky, A.E. Photophysical properties of BODIPYs with sterically-hindered nitrophenyls in meso-position. *J. Lumin.* **2022**, *246*, 118837. [CrossRef]

27. Bettinger, H.F.; Rabuck, A.D.; Scuseria, G.E.; Wang, N.-X.; Litosh, V.A.; Saini, R.K.; Billups, W.E. Pathways for the thermally induced dehydrogenation of $C_{60}H_2$. *Chem. Phys. Lett.* **2002**, *360*, 509–514. [CrossRef]
28. Sunahara, H.; Urano, Y.; Kojima, H.; Nagano, T. Design and synthesis of a library of BODIPY-based environmental polarity sensors utilizing photoinduced electron-transfer-controlled fluorescence ON/OFF switching. *J. Am. Chem. Soc.* **2007**, *129*, 5597–5604. [CrossRef]
29. Słowiński, D.; Świerczyńska, M.; Romański, J.; Podsiadły, R. Sensitive Detection of Various Forms of Hydrogen Sulfide via Highly Selective Naphthalimide-Based Fluorescent Probe. *Molecules* **2023**, *28*, 6299. [CrossRef]
30. Lippert, A.R.; New, E.J.; Chang, C.J. Reaction-based fluorescent probes for selective imaging of hydrogen sulfide in living cells. *J. Am. Chem. Soc.* **2011**, *133*, 10078–10080. [CrossRef]
31. Saha, T.; Kand, D.; Talukdar, P. A colorimetric and fluorometric BODIPY probe for rapid, selective detection of H_2S and its application in live cell imaging. *Org. Biomol. Chem.* **2013**, *11*, 8166–8170. [CrossRef] [PubMed]
32. Zheng, K.; Lin, W.; Tan, L. A phenanthroimidazole-based fluorescent chemosensor for imaging hydrogen sulfide in living cells. *Org. Biomol. Chem.* **2012**, *10*, 9683–9688. [CrossRef] [PubMed]
33. Yang, L.; Zhang, Y.; Ren, X.; Wang, B.; Yang, Z.; Song, X.; Wang, W. Fluorescent Detection of Dynamic H_2O_2/H_2S Redox Event in Living Cells and Organisms. *Anal. Chem.* **2020**, *92*, 4387–4394. [CrossRef] [PubMed]
34. Wen, Y.; Liu, K.; Yang, H.; Li, Y.; Lan, H.; Liu, Y.; Zhang, X.; Yi, T. A highly sensitive ratiometric fluorescent probe for the detection of cytoplasmic and nuclear hydrogen peroxide. *Anal. Chem.* **2014**, *86*, 9970–9976. [CrossRef] [PubMed]
35. Pak, Y.L.; Park, S.J.; Xu, Q.; Kim, H.M.; Yoon, J. Ratiometric Two-Photon Fluorescent Probe for Detecting and Imaging Hypochlorite. *Anal. Chem.* **2018**, *90*, 9510–9514. [CrossRef] [PubMed]
36. Manatt, S.L.; Manatt, M.R. On the analyses of mixture vapor pressure data: The hydrogen peroxide/water system and its excess thermodynamic functions. *Chem. Eur. J.* **2004**, *10*, 6540–6557. [CrossRef]
37. Xu, M.; Han, J.M.; Zhang, Y.; Yang, X.; Zang, L. A selective fluorescence turn-on sensor for trace vapor detection of hydrogen peroxide. *Chem. Commun.* **2013**, *49*, 11779–11781. [CrossRef]
38. Matsumoto, A.; Nishiyabu, R.; Kubo, Y. Synthesis of a borylated boron–dibenzopyrromethene dye enabling the visual detection of H_2O_2 vapor. *RSC Adv.* **2014**, *4*, 37973–37978. [CrossRef]

Disclaimer/Publisher's Note: The statements, opinions and data contained in all publications are solely those of the individual author(s) and contributor(s) and not of MDPI and/or the editor(s). MDPI and/or the editor(s) disclaim responsibility for any injury to people or property resulting from any ideas, methods, instructions or products referred to in the content.